VIP Nanoparticles

DOI: 10.1002/anie.200804238

Core–Multishell Magnetic Coordination Nanoparticles: Toward Multifunctionality on the Nanoscale**

Laure Catala, Daniela Brinzei, Yoann Prado, Alexandre Gloter, Odile Stéphan, Guillaume Rogez, and Talal Mallah**

Three-dimensional Prussian Blue analogues (PBAs) and related cyano-bridged coordination networks have been at the forefront of the field of molecular magnetism for more than a decade because of the extraordinary variety of their physical properties (electrochromism, ferromagnetism, photomagnetism, piezomagnetism, spin crossover), which opens up prospects for original functional materials.[1–13] The large metal–metal distance (≈ 5 Å) across the cyano bridge leads to relatively large porosity, which may play a role in hydrogen storage, ion selection, catalysis, and sensors.[13,14] One important issue is the effect of size reduction on the physical and chemical behavior of cyano-bridged coordination networks and their possible application as molecule-based components in devices.[11,15,16] A unique way to take advantage of the physical behavior of PBAs stemming from their rich electronic properties and porosity is to synthesize multishell nanoparticles such that a single particle consists of a core of a given network surrounded by shells of networks that may contain other functionalities. We report here the design of core–multishell nanocrystals thanks to the stabilization of surfactant-free particles in water. Epitaxial growth of different shells on various charged cores is demonstrated, and the thickness of the shells can be fine-tuned. The synergy between the different components is illustrated with one selected magnetic core–shell system.

During the last few years, several groups have attempted to establish chemical routes that allow the stabilization of coordination (or metal–organic) nanoparticles of various face-centered-cubic PBAs of the general formula $A^{I}_{x}M^{II}[M'^{III}(CN)_6]_{(2+x)/3}$, where A is an alkali-metal cation and M^{II} and M'^{III} are transition-metal ions (see the Supporting Information). Generally, a chemical agent (organic or inorganic) is used during the synthetic process to control the growth of the particles, preclude their aggregation, and ensure their dispersion in different solvents.[15–31] However, the presence of such protective agents weakens, in most cases, the surface reactivity of the particles and their electronic coupling with other objects, consequently decreasing their multifunctional potential. This can be avoided by the stabilization in solution of surfactant-free nanoparticles. We have recently shown that such electrostatic stabilization can be achieved in the case of the $Cs^{I}[Ni^{II}Cr^{III}(CN)_6]$ network leading to quasi-monodisperse particles with a size of 6.5 nm in diameter.[32] The stabilization of surfactant-free nanoparticles makes it possible to perform coordination chemistry on the particles' surface and opens the possibility of the epitaxial growth of one or several shells on the preexisting cores in solution. Thus, the key requirement for the preparation of pure core–shell nanoparticles is 1) stabilization in solution of well-defined crystalline surfactant-free charged nanoparticles and 2) prevention of the side nucleation of the shell by controlling the addition rate and the concentration of the components. Inorganic multishell particles have been prepared on oxides, sulfides, and metallic cores; some interesting examples of shape control have been reported by epitaxial growth seed-mediated procedures involving surfactants.[33,34] However, this is the first example of core-multishell particles based on coordination networks.

The general procedure for the simple growth process on the charged cores present in solution is straightforward and thus feasible on a large scale: a dilute solution containing the divalent metal salt ($M(H_2O)_6Cl_2$) and CsCl, and another containing the hexacyanometalate(III) salt are added dropwise ($1\ mL\,s^{-1}$) to a stirred solution containing the core particles. The thickness of the growing shell is finely controlled by adjusting the amount of material added in solution (see the Supporting Information). As the growth process occurs, the solution is diluted in order to avoid aggregation that may occur because of the increase of the ionic force.

To show the versatility and the efficiency of this approach, we report the preparation and the characterization of surfactant-free $Cs^{I}[Fe^{II}Cr^{III}(CN)_6]$ and $Cs^{I}[Co^{II}Cr^{III}(CN)_6]$ nanoparticles as well as the design of core–(multi)shell particles of three different systems: 1) bicomponent particles made of a shell of $Co^{II}[Cr^{III}(CN)_6]_{2/3}$ on top of the $Cs^{I}[Fe^{II}Cr^{III}(CN)_6]$ core (denoted CsFeCr@CoCr), 2) tricomponent particles made of two different shells of $Cs^{I}[Fe^{II}Cr^{III}(CN)_6]$ and then $Cs^{I}[Ni^{II}Cr^{III}(CN)_6]$ grown on

[*] Dr. L. Catala, Dr. D. Brinzei, Y. Prado, Prof. T. Mallah
Institut de Chimie Moléculaire et des Matériaux d'Orsay
Université Paris-Sud 11, 91405 Orsay (France)
Fax: (+33) 1-6915-4754
E-mail: laurecatala@icmo.u-psud.fr
mallah@icmo.u-psud.fr

Dr. A. Gloter, Prof. O. Stéphan
Laboratoire de Physique des Solides, Université Paris-Sud 11
91405 Orsay (France)

Dr. G. Rogez
IPCMS-GMI, UMR CNRS 7504, 23, rue du Loess, B.P. 43
67034 Strasbourg Cedex 2 (France)

[**] We thank the CNRS (Centre National de la Recherche Scientifique), the French program ANR-blanc (project MS-MCNP), and the European Community (contract MRTN-CT-2003-504880/RTN Network "QuEMolNa", contract NMP3-CT-2005-515767 NoE "MAGMANET") for financial support.

Supporting information for this article is available on the WWW under http://dx.doi.org/10.1002/anie.200804238.

top of a $Cs^{I}[Co^{II}Cr^{III}(CN)_6]$ core (denoted CsCoCr@CsFeCr@CsNiCr), and 3) bicomponent particles of a $Cs^{I}[Co^{II}Cr^{III}(CN)_6]$ shell on top of the $Cs^{I}[Ni^{II}Cr^{III}(CN)_6]$ core ($d = 6.5$ nm), which we recently reported elsewhere[32] (denoted CsNiCr@CsCoCr). In order to evidence the multishell structure by scanning electron transmission microscopy (STEM) and electron energy loss spectroscopy (EELS), relatively large cores and shells (larger than 10 nm) were employed for CsFeCr@CoCr and CsCoCr@CsFeCr@CsNiCr. The third example was elaborated starting from smaller and more homogeneous cores, that is, the quasi-monodisperse $Cs^{I}Ni^{II}Cr^{III}(CN)_6$ particles ($d = 6.5$ nm). In order to recover the particles as dispersible powders and to perform the different characterization and the magnetic studies, we systematically coated the water-soluble nanostructures with dioctadecyl dimethyl ammonium (DODA).

We elaborated the bicomponent particles (CsFeCr@CoCr) on a polydisperse sample of CsFeCr particles used as cores in order to validate the method by checking that the growth of the shell occurs on all the cores and that no side reaction occurs. The sample was characterized by transmission electronic microscopy (TEM) (Figure S1 in the Supporting Information) and by high-resolution transmission electronic microscopy (HRTEM) (Figure 1). A perfect

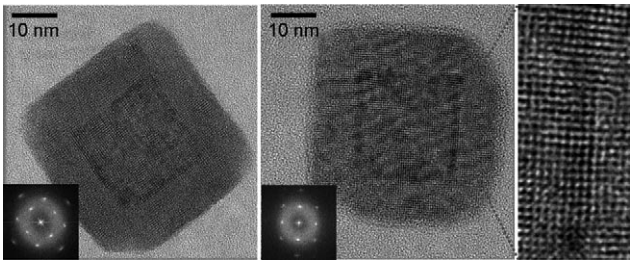

Figure 1. HRTEM images of two core–shell CsFeCr@CoCr nanoparticles and diffractogram patterns showing a face-centered cubic structure; the shorter distance is 5.2 Å and corresponds to the (200) planes of the *fcc* structure (left). In the enlarged image on the right the (100) interface between the core and shell shows the perfect epitaxy of the two components.

matching of the two networks is observed, demonstrating the epitaxial growth of the CoCr shell network on the CsFeCr core. The pattern in the diffractogram with fourfold symmetry (Figure 1, insert) confirms the cubic structure of the nanoparticles. The lattice spacing between the neighboring fringes (measured at around 5.2 Å) is in agreement with an *fcc* cell parameter of 10.5 Å, as is also the case for PBA. Chemical imaging of the core–shell particles by STEM in high angular dark field mode (HAADF-STEM) and in EELS mode (Figure 2) confirms that Cr, N, and C are present throughout the entire particle while Fe is present only at the center of the core–shell particle. Since when the core is probed the shell is probed simultaneously, the contrast due to the Co atoms cannot be zero in the core; however, the contrast of Co must be much larger at the periphery. This is what we observe in Figure 2. The core–shell structure is proved by the Fe chemical map, which shows that Fe is present exclusively in

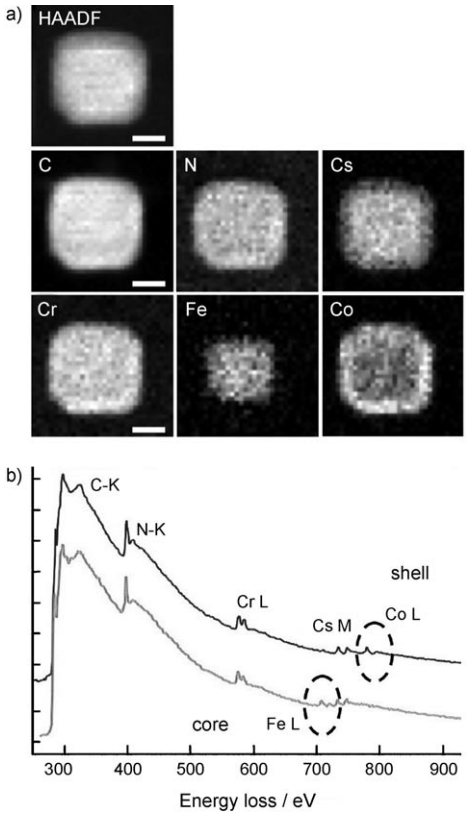

Figure 2. a) STEM-HAADF and STEM-EELS chemical maps of a CsFeCr@CoCr core–shell particle (scale bars: 20 nm). b) Comparison between the EELS spectra of the core and shell parts of a CsFeCr@CoCr particle. The C *K*, N *K*, Cr *L*2,3, Fe *L*2,3, Cs *M*4,5, and Co *L*2,3 edges can be seen at 285, 402, 575, 710, 726, and 779 eV, respectively.

the core. Cs is present in the core as expected but also in the shell since Cs^+ was introduced in excess during the synthesis of the core nanoparticles and was still present in solution when the shell assembled. The Cs^+ concentration in the shell is lower, which explains the lower contrast observed on both HRTEM and HAADF-STEM images (see Figures 1 and 2 and the Supporting Information). More importantly, homogeneous coverage was obtained independent of the size of the starting core particles, as seen on the chemical mapping of an assembly of particles (Figure S2 in the Supporting Information). Neither residual (not covered by a shell) CsFeCr core particles were observed nor new CoCr particles were formed in solution. The analysis of the size of the different particles is in excellent agreement with the predicted size (Figure S2 in the Supporting Information). The IR spectra of the DODA-protected particles show the characteristic bands of both components (Table S1 in the Supporting Information).

To give further evidence of the versatile synthesis of core–multishell coordination nanoparticles, the three-component system CsCoCr@CsFeCr@CsNiCr containing networks with three different divalent metal ions was elaborated: first CsCoCr core particles with a mean size of (12.1 ± 2.9) nm were obtained spontaneously as charged particles in water (Figure S3a in the Supporting Information), then two different shells of CsFeCr and CsNiCr were grown sequentially. To

do so, we added the calculated amount of the precursors following the same general procedure (see the Supporting Information), and we monitored the growth process by dynamic light scattering (DLS; see Figure S4 in the Supporting Information) and TEM. DLS measurements confirm that during the growth process, only particles of one mean size are present in solution: no smaller unreacted particles are present, and no particles with a size different from that expected are formed in the growth process. The intermediate CsCoCr@CsFeCr particles have a mean aspect ratio of 1.15 ((30.2 ± 8.4) nm $\times$ (26.2 ± 7.1) nm) as observed by TEM (Figure S3b in the Supporting Information), and the three-shell particles maintain almost the same aspect ratio (1.1) with a mean length of (51.1 ± 8.1) nm and a width of (46.3 ± 6.6) nm (Figure S3c in the Supporting Information). The small aspect ratio observed for the core nanoparticles reflects the shape of the nuclei formed during the nucleation step which appears not to be cubic. Kinetic studies to investigate the very first steps of the nucleation process are underway.

The crystallinity of the core and the first shell were confirmed by HRTEM imaging (Figure 3d). The outer shell appears amorphous probably because it was damaged by the beam during observation, as shown by the progressive disappearance of the lattice fringes under irradiation (Figure S5 in the Supporting Information). X-ray powder diffraction was performed and it confirmed the *fcc* structure of the particles (Table S2); in the IR spectrum the characteristic asymmetric vibrations of the cyano groups evidence their presence in the three components (Table S1 in the Supporting Information). The EELS chemical profiles confirm clearly the multicomponent nature of the nanoparticles, with cobalt located in the core, iron absent in the outer shell, and nickel exclusively in the outer shell, while Cr is found everywhere (Figure 3a). Images of a collection of particles by HAADF-STEM confirm the homogeneity of the reaction. Full coverage of all the core particles occurs, and a weak contrast is observed between the three layers (Figure S6). Despite the theoretical lability of the metal complexes on the particles' surface, diffusion of the shell metal ions in the core was not detected by EELS mapping (1 nm resolution). This is probably because of the large thermodynamic stability of the surface molecules resulting from the template effect imposed by the particle.

Core–multishell magnetic nanoparticles made of three different networks, which may have different properties, can thus be designed. Once the feasibility of the procedure was established on rather large nanoparticles by STEM-EELS experiments, the method was applied starting from much the smaller and homogenous CsNiCr nanoparticles ($d = 6.5$ nm) already reported and characterized.[32] Two types of particles with the same size (12–13 nm) were prepared: core–shell CsNiCr@CsCoCr and a pure CsNiCr. The core–shell CsNiCr@CsCoCr particles were prepared as follows: first a shell of the CsNiCr network was grown on top of the CsNiCr particles ($d = 6.5$ nm) to achieve 9 nm CsNiCr particles, and then another shell of CsCoCr of 1.5 nm thickness was grown on top of these particles to give CsNiCr@CsCoCr two-component objects with a diameter of 12 nm ($9 + 2 \times 1.5$ nm). The growth of the particles was monitored by DLS measurements (Figure S7 in the Supporting Information), which give evidence of the successful growth process without any side reactions or rearrangements in solution. Secondly, pure CsNiCr particles of the same size ($d = 12$–13 nm) were synthesized by growing a shell of CsNiCr on the CsNiCr particles ($d = 6.5$ nm). A portion of each of the three samples (9 nm CsNiCr, 12 nm CsNiCr, and 12 nm CsNiCr@CsCoCr) was treated with DODA-Br to provide a concentrated sample suitable for routine characterization; another portion was treated with polyvinylpyrrolidone (PVP) to obtain samples of the particles highly dispersed in an organic polymer suitable for magnetic characterization.

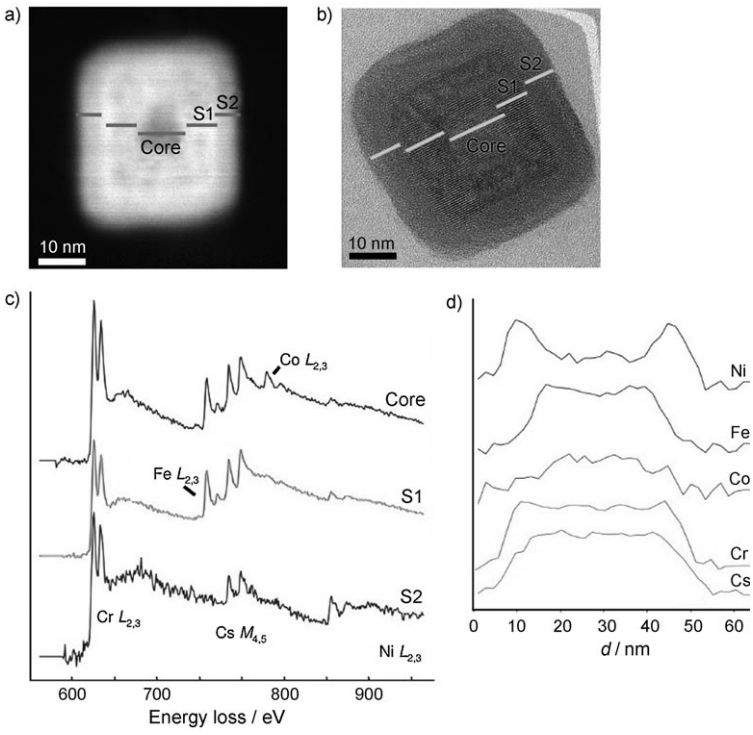

Figure 3. HAADF-STEM (a) and HRTEM (b) images of a CsCoCr@CsFeCr@CsNiCr particle. c) Comparison between the EELS spectra of the core and shell parts (S1 and S2) of the particle. d) A line profile across another particle shows that Cr and Cs are present throughout the whole particle while Co, Fe, Ni are only in domains.

TEM images reveal a mean size of $d = (9.4 \pm 2.1)$ nm for the DODA-protected CsNiCr particles (Figure S8a), (12.9 ± 2.6) nm for the CsNiCr particles (Figure S8b), and (12.5 ± 1.7) nm for the CsNiCr@CsCoCr particles (Figure S9 in the Supporting Information). The particles have thus been obtained with a rather homogeneous size for the three samples, and more importantly in very good agreement with the predicted size. The size of the core–multishell particles can thus be fine-tuned by adding a calculated amount of material. HRTEM studies on the CsNiCr@CsCoCr particles (Figure 4a) show no difference in contrast between the core and the shell, attesting to their excellent

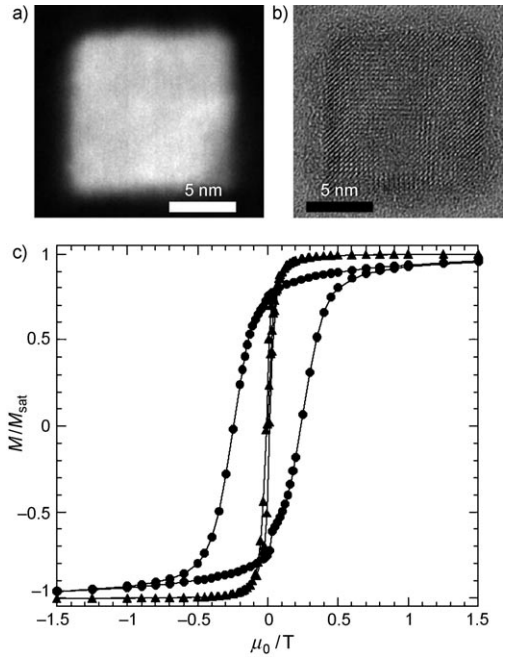

Figure 4. HAADF-STEM (a) HRTEM (b) images of a CsNiCr@CsCoCr particle ($d = 12$ nm). c) Plot of magnetization versus field for CsNiCr@CsCoCr particles (circles) and CsNiCr particles ($d = 12$ nm; triangles).

crystallinity as a result of the perfect matching of the core and the grown shells.

Magnetic measurements were performed on the PVP-diluted particles, in alternating current and direct current modes. A frequency-dependent out-of-phase susceptibility signal is observed for the CsNiCr particles ($d = 9.4$ nm) with a maximum around 12 K (Figure S10 in the Supporting Information). The core–shell CsNiCr@CsCoCr particles have similar behavior but with a maximum around 35 K (Figure S10). The absence of a maximum around 12 K in the analogous studies of the CsNiCr@CsCoCr particles is consistent with a homogenous and full coverage of all the core particles present in the sample. The efficiency of the growth of a shell with a thickness of 1.5 nm (from d = 9.4 to 12.4 nm), which corresponds to three single layers, is demonstrated. Magnetization versus applied field was plotted for the CsNiCr, CsCoCr, and CsNiCr@CsCoCr particles with diameters of 12–13 nm. A large hysteresis cycle with a coercive field of 2500 Oe was observed for the core–shell CsNiCr@CsCoCr particles, while much weaker coercive fields were found for the pure particles: 80 and 600 Oe for CsNiCr and CsCoCr, respectively (Figure 4c and Figure S11 in the Supporting Information). The presence of a thin shell (1.5 nm, roughly three molecular layers) containing anisotropic Co^{II} ions on top of the less anisotropic CsNiCr particles induces a large surface anisotropy which is responsible for the coercive field enhancement; this demonstrates the synergistic effect of the core-shell structure on magnetic behavior.

We have synthesized core–multishell nanoparticles of various cyano-bridged coordination networks by epitaxial growth in solution. Precise control over the shell thickness was achieved, which allows fine-tuning of the particles' size and their magnetic anisotropy. Size-reduction effects on functional cyano-based networks that exhibit electrochromism, magnetism, spin crossover, photomagnetism, or thermally induced charge transfer may now be easily examined on the nanoscale since shells of any network and of controlled thickness can be grown on any desired core; in this way different properties can be combined in a single nano-object. Multifunctional nanoparticles that may be addressed by different external stimuli (electric field, magnetic field, light, temperature, pressure) may now be prepared, leading to useful functional (and eventually multifunctional) objects on the nanoscale. Moreover, as no organic or inorganic agents are required, this straightforward preparation of core–multishell particles can be further exploited for their organization on surfaces as mono- and multilayers,[35,36] and more importantly as components in functional devices.

Received: August 27, 2008
Published online: November 26, 2008

Keywords: coordination networks · core–shell structures · magnetic properties · nanoparticles · nanostructures

[1] T. Mallah, S. Thiebaut, M. Verdaguer, P. Veillet, *Science* **1993**, *262*, 1554.
[2] W. R. Entley, G. S. Girolami, *Science* **1995**, *268*, 397.
[3] S. Ferlay, T. Mallah, R. Ouahes, P. Veillet, M. Verdaguer, *Nature* **1995**, *378*, 701.
[4] O. Sato, T. Iyoda, A. Fujishima, K. Hashimoto, *Science* **1996**, *272*, 704.
[5] Y. Sato, S. Ohkoshi, K. Arai, M. Tozawa, K. Hashimoto, *J. Am. Chem. Soc.* **2003**, *125*, 14590.
[6] J. S. Miller, J. L. Manson, *Acc. Chem. Res.* **2001**, *34*, 563.
[7] S. Ohkoshi, H. Tokoro, T. Hozumi, Y. Zhang, K. Hashimoto, C. Mathoniere, I. Bord, G. Rombaut, M. Verelst, C. C. D. Moulin, F. Villain, *J. Am. Chem. Soc.* **2006**, *128*, 270.
[8] O. Sato, *J. Solid State Electrochem.* **2007**, *11*, 773.
[9] W. Kosaka, K. Nomura, K. Hashimoto, S. I. Ohkoshi, *J. Am. Chem. Soc.* **2005**, *127*, 8590.
[10] E. Coronado, M. C. Gimenez-Lopez, G. Levchenko, F. M. Romero, V. Garcia-Baonza, A. Milner, M. Paz-Pasternak, *J. Am. Chem. Soc.* **2005**, *127*, 4580.
[11] S. Bonhommeau, G. Molnar, A. Galet, A. Zwick, J. A. Real, J. J. McGarvey, A. Bousseksou, *Angew. Chem.* **2005**, *117*, 4137; *Angew. Chem. Int. Ed.* **2005**, *44*, 4069.
[12] V. Niel, J. M. Martinez-Agudo, M. C. Munoz, A. B. Gaspar, J. A. Real, *Inorg. Chem.* **2001**, *40*, 3838.
[13] N. R. de Tacconi, K. Rajeshwar, R. O. Lezna, *Chem. Mater.* **2003**, *15*, 3046.
[14] S. S. Kaye, J. R. Long, *J. Am. Chem. Soc.* **2005**, *127*, 6506.
[15] L. Catala, T. Gacoin, J. P. Boilot, E. Riviere, C. Paulsen, E. Lhotel, T. Mallah, *Adv. Mater.* **2003**, *15*, 826.
[16] D. Brinzei, L. Catala, C. Mathoniere, W. Wernsdorfer, A. Gloter, O. Stephan, T. Mallah, *J. Am. Chem. Soc.* **2007**, *129*, 3778.
[17] S. P. Moulik, G. C. De, A. K. Panda, B. B. Bhowmik, A. R. Das, *Langmuir* **1999**, *15*, 8361.
[18] S. Vaucher, M. Li, S. Mann, *Angew. Chem.* **2000**, *112*, 1863; *Angew. Chem. Int. Ed.* **2000**, *39*, 1793.
[19] J. M. Dominguez-Vera, E. Colacio, *Inorg. Chem.* **2003**, *42*, 6983.
[20] G. Romualdo-Torres, B. Agricole, C. Mingotaud, S. Ravaine, P. Delhaes, *Langmuir* **2003**, *19*, 4688.
[21] T. Uemura, S. Kitagawa, *J. Am. Chem. Soc.* **2003**, *125*, 7814.

[22] J. G. Moore, E. J. Lochner, C. Ramsey, N. S. Dalal, A. E. Stiegman, *Angew. Chem.* **2003**, *115*, 2847; *Angew. Chem. Int. Ed.* **2003**, *42*, 2741.
[23] E. Dujardin, S. Mann, *Adv. Mater.* **2004**, *16*, 1125.
[24] L. Catala, C. Mathoniere, A. Gloter, O. Stephan, T. Gacoin, J. P. Boilot, T. Mallah, *Chem. Commun.* **2005**, 746.
[25] T. Uemura, S. Kitagawa, *Chem. Lett.* **2005**, *34*, 132.
[26] L. Catala, A. Gloter, O. Stephan, G. Rogez, T. Mallah, *Chem. Commun.* **2006**, 1018.
[27] Y. Guari, J. Larionova, K. Molvinger, B. Folch, C. Guerin, *Chem. Commun.* **2006**, 2613.
[28] W. Kosaka, M. Tozawa, K. Hashimoto, S. I. Ohkoshi, *Inorg. Chem. Commun.* **2006**, *9*, 920.
[29] M. Arai, M. Miyake, M. Yamada, *J. Phys. Chem. C* **2008**, *112*, 1953.
[30] E. Chelebaeva, Y. Guari, J. Larionova, A. Trifonov, C. Guerin, *Chem. Mater.* **2008**, *20*, 1367.
[31] B. Folch, Y. Guari, J. Larionova, C. Luna, C. Sangregorio, C. Innocenti, A. Caneschi, C. Guerin, *New J. Chem.* **2008**, *32*, 273.
[32] D. Brinzei, L. Catala, N. Louvain, G. Rogez, O. Stephan, A. Gloter, T. Mallah, *J. Mater. Chem.* **2006**, *16*, 2593.
[33] E. S. Habas, H. Lee, V. Radmilovic, G. A. Somorjai, P. Yang, *Nat. Mater.* **2007**, *6*, 692.
[34] F.-R. Fan, D.-Y. Liu, Y.-F. Wu, S. Duan, Z.-X. Xie, Z.-Y. Jiang, Z.-Q. Tian, *J. Am. Chem. Soc.* **2008**, *130*, 6469.
[35] M. Clemente-Leon, E. Coronado, A. Lopez-Munoz, D. Repetto, C. Mingotaud, D. Brinzei, L. Catala, T. Mallah, *Chem. Mater.* **2008**, *20*, 4642.
[36] B. Fleury, F. Volatron, L. Catala, D. Brinzei, E. Rivière, V. Huc, C. David, F. Miserque, G. Rogez, L. Baraton, S. Palacin, T. Mallah, *Inorg. Chem.* **2008**, *47*, 1898.

